QCL-based nonlinear sensing of independent targets dynamics

QCL-based nonlinear sensing of independent targets dynamics

F. P. Mezzapesa,[1,2,*] L. L. Columbo,[1,3] M. Dabbicco,[1,2] M. Brambilla,[1,2] and G. Scamarcio[1,2]

[1]*CNR-IFN UOS Bari, via Amendola 173, I-70126 Bari, Italy*
[2]*Dipartimento Interateneo di Fisica, Università degli Studi e Politecnico di Bari, via Amendola 173, I-70126 Bari, Italy*
[3]*Dipartimento di Scienza ed Alta tecnologia, Università dell'Insubria,via Valleggio 11, 22100 Como, Italy*
[*]*francesco.mezzapesa@uniba.it*

Abstract: We demonstrate a common-path interferometer to measure the independent displacement of multiple targets through nonlinear frequency mixing in a quantum-cascade laser (QCL). The sensing system exploits the unique stability of QCLs under strong optical feedback to access the intrinsic nonlinearity of the active medium. The experimental results using an external dual cavity are in excellent agreement with the numerical simulations based on the Lang-Kobayashi equations.

OCIS codes: (140.5965) Semiconductor lasers, quantum cascade; (190.4223) Nonlinear wave mixing; (280.3420) Laser sensors; (280.4788) Optical sensing and sensors; (120.3180) Interferometry.

References and links

1. F. P. Mezzapesa, L. L. Columbo, M. Brambilla, M. Dabbicco, S. Borri, M. S. Vitiello, H. E. Beere, D. A. Ritchie, and G. Scamarcio, "Intrinsic stability of quantum cascade lasers against optical feedback," Opt. Express **21**(11), 13748–13757 (2013).
2. J. von Staden, T. Gensty, W. Elsässer, G. Giuliani, and C. Mann, "Measurements of the alpha factor of a distributed-feedback quantum cascade laser by an optical feedback self-mixing technique," Opt. Lett. **31**(17), 2574–2576 (2006).
3. R. P. Green, J. H. Xu, L. Mahler, A. Tredicucci, F. Beltram, G. Giuliani, H. E. Beere, and D. A. Ritchie, "Linewidth enhancement factor of terahertz quantum cascade lasers," Appl. Phys. Lett. **92**(7), 071106 (2008).
4. M. C. Phillips and M. S. Taubman, "Intracavity sensing via compliance voltage in an external cavity quantum cascade laser," Opt. Lett. **37**(13), 2664–2666 (2012).
5. P. Dean, Y. L. Lim, A. Valavanis, R. Kliese, M. Nikolić, S. P. Khanna, M. Lachab, D. Indjin, Z. Ikonić, P. Harrison, A. D. Rakić, E. H. Linfield, and A. G. Davies, "Terahertz imaging through self-mixing in a quantum cascade laser," Opt. Lett. **36**(13), 2587–2589 (2011).
6. F. P. Mezzapesa, V. Spagnolo, A. Antonio, and G. Scamarcio, "Detection of ultrafast laser ablation using quantum cascade laser-based sensing," Appl. Phys. Lett. **101**(17), 171107 (2012).
7. Y. L. Lim, P. Dean, M. Nikolic, R. Kliese, S. P. Khanna, M. Lachab, A. Valavanis, D. Indjin, Z. Ikonic, P. Harrison, E. Linfield, A. G. Davies, S. J. Wilson, and A. D. Rakic, "Demonstration of a self-mixing displacement sensor based on terahertz quantum cascade lasers," Appl. Phys. Lett. **99**(8), 081108 (2011).
8. S. Ottonelli, F. De Lucia, M. Di Vietro, M. Dabbicco, G. Scamarcio, and F. P. Mezzapesa, "A compact three degrees-of-freedom motion sensor based on the laser-self-mixing effect," IEEE Photon. Technol. Lett. **20**(16), 1360–1362 (2008).
9. X. Dai, M. Wang, and C. Zhou, "Multiplexing self-mixing interference in fiber ring lasers," IEEE Photon. Technol. Lett. **22**(21), 1619–1621 (2010).
10. Y. L. Lim, R. Kliese, K. Bertling, K. Tanimizu, P. A. Jacobs, and A. D. Rakić, "Self-mixing flow sensor using a monolithic VCSEL array with parallel readout," Opt. Express **18**(11), 11720–11727 (2010).
11. F. P. Mezzapesa, L. Columbo, M. Brambilla, M. Dabbicco, A. Ancona, T. Sibillano, F. De Lucia, P. M. Lugarà, and G. Scamarcio, "Simultaneous measurement of multiple target displacements by self-mixing interferometry in a single laser diode," Opt. Express **19**(17), 16160–16173 (2011).
12. F. Zhao, "Sub-aperture interferometers: multiple target sub-beams are derived from the same measurement beam," NASA Tech Briefs. **29–30** (2010).
13. R. Juskaitis, N. P. Rea, and T. Wilson, "Semiconductor laser confocal microscopy," Appl. Opt. **33**(4), 578–584 (1994).
14. S. Shinohara, A. Mochizuki, H. Yoshida, and M. Sumi, "Laser Doppler velocimeter using the self-mixing effect of a semiconductor laser diode," Appl. Opt. **25**(9), 1417–1419 (1986).

#201073 - $15.00 USD Received 8 Nov 2013; revised 1 Jan 2014; accepted 21 Jan 2014; published 6 Mar 2014

15. R. Lang and K. Kobayashi, "External optical feedback effects on semiconductor injection laser properties," IEEE J. Quantum Electron. **16**(3), 347–355 (1980).
16. M. Wang and G. Lai, "Self-mixing microscopic interferometer for the measurement of micro-profile," Opt. Commun. **238**(4–6), 237–244 (2004).

1. Introduction

Recently, we have shown that quantum cascade laser (QCL) sensors based on optical feedback interferometry are mostly attractive owing to the intrinsic stability of the QCL continuous wave (CW) emission in presence of optical reinjection [1]. In fact, QCLs do tolerate strong optical feedback without exhibiting dynamical instabilities typical of bipolar semiconductor lasers, such as mode-hopping, intensity pulsation or coherence collapse. This unique behaviour of QCLs can be ascribed to i) the ultrafast intersubband relaxation time (i.e. the high value of the photon-to-carrier lifetime ratio), which prevents the destabilization via undamped relaxation oscillations, and ii) the smaller linewidth enhancement factor (LEF) with respect to conventional diode lasers, that reduces the number of external cavity modes possibly concurring in destabilizing the CW emission.

Moreover, the inherent sensitivity of the QCL compliance voltage to the optical feedback is particularly suitable in self-mixing (SM) schemes [2, 3], since the power modulation can be detected directly as the voltage modulation at the laser junction with no need of external detectors. In fact, mid-infrared (MIR) and terahertz QCLs are the best alternative to diode lasers in contactless metrology and engineering applications where the wavelength agility, spectral purity and high output power associated with QCLs are required. So far, phase spectroscopy [4], imaging [5], in-line laser ablation monitoring [6], and target displacement measurements [7] have been demonstrated. Specifically, in the latter case the analysis of the self-mixing interferogram has been used to measure a single degree-of-freedom of a moving object obscured by opaque materials. To monitor multiple points on the same target surface, simultaneous interferometric channels were needed, as already reported [8–10]. However, this solution often required custom multisource assemblies and specific design of laser cavities.

As a significant step in this direction we have recently reported an all-optical sensor based on SM interferometry in a single laser diode which was capable to concurrently measure the independent displacement of individual sections of a target [11]. Particularly, the experimental validation of this sensing technique was given during ultrafast laser percussion drilling, thus demonstrating that the interferometric sensor could accurately monitor the displacement of the ablation front of an otherwise static target.

In the following, we demonstrate a novel application of the optical feedback interferometry in a single QCL to measure the collinear displacement of independently moving targets through nonlinear frequency mixing into the laser cavity. The main advantage of QCLs is given by their high stability against optical feedback, which allows for virtually perfect common-mode rejection. The working principle is inspired by the wavefront-split interferometry, also known as sub-aperture interferometry, which has been mainly employed in astronomy [12]. Simultaneously measuring displacements of multiple targets can be achieved by splitting the wavefront of the measurement beam into sub-beams, which are in turn aimed at different retro-reflecting targets. The common-path geometry and the laser self-mixing scheme both allows for an extremely compact and self-aligned multiparametric interferometer as the QCL incorporate the detector functionality within the laser cavity itself .

2. Experimental results

We consider the experimental setup sketched in Fig. 1. The SM measuring system is based on a tunable single mode MIR quantum cascade laser working at $\lambda \approx 6.24$ μm and temperature stabilized at 10° C. To maximize the sensitivity to optical feedback, the QCL was driven slightly above the threshold (i.e. i_{th} = 486.5 mA for the solitary QCL) at constant current i = 490 mA. The highly divergent beam from the QCL was collimated by an AR-coated

#201073 - $15.00 USD Received 8 Nov 2013; revised 1 Jan 2014; accepted 21 Jan 2014; published 6 Mar 2014

chalcogenide glass aspheric lens having numerical aperture NA = 0.56 and nominal focal length of 4 mm.

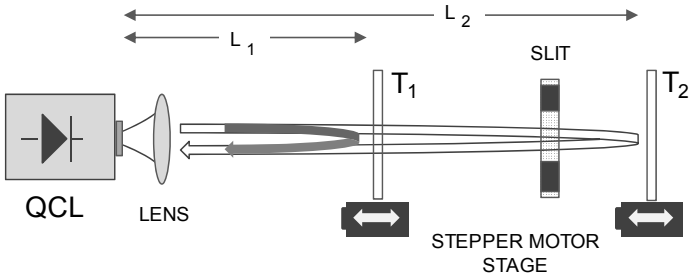

Fig. 1. Schematic layout of the experimental setup, showing two independent targets (T_1 and T_2) on the translation stages. The two targets are transparent film of polypropylene.

The dual external cavity was composed of two identical polypropylene sheets (17% reflectance), collinearly aligned along the optical axis at a distance of 300 mm and 550 mm from the QCL, respectively, and mounted onto motorized linear stages. A fraction of the optical field is coupled back to the lasing mode within the active cavity after reflection from the specimens T_1 and T_2. A variable aperture placed in between T_1 and T_2 allowed to adjust the effective optical feedback off the front surface of T_2. The light-current curves for a solitary QCL and the same laser with optical feedback from the two targets, show a fractional reduction of the effective threshold with increasing the level of back-injected radiation in the laser cavity, as expected [13]. The coherent feedback signal perturbing the laser emission was revealed as modulations of the junction voltage while the QCL was driven in the CW mode operation. The self-mixing interferograms exhibited conventional asymmetric waveforms (i.e. saw-tooth like fringes) with fast switching each time the interferometric phase was varied by 2π. The junction voltage offset measured across the device was subtracted by ac-coupling to a low noise amplifier and then Fourier transformed by a digital oscilloscope. The Fourier transform of the SM signal from a moving target allows the extraction of the Doppler shifted frequency of the backscattered radiation as the beating modulation of the emitted power [14].

Figure 2 shows experimental time-domain SM signals for different optical configurations. The top trace was recorded with the target T_1 moving at a constant velocity $v_1 = 0.5$ mm/s directed away from the laser source, while the target T_2 remained stationary. The resulting fringe period in Fig. 2(a) (i.e. the frequency of a mode hop in the external cavity) corresponds to a target displacement of $\lambda/2$ and the motion direction can be resolved from the polarity of sharp pulses in the analogue derivative of the SM signal, as shown in the upper trace of Fig. 2(b). Figure 2(c) shows the normalized power spectrum of the laser self-mixing signal from the dual cavity. The top trace in Fig. 2(c) contains a low frequency peak at $\omega_1 = 4\pi v_1/\lambda \approx 1$ kHz and its harmonics at about 2 and 3 kHz.

#201073 - $15.00 USD Received 8 Nov 2013; revised 1 Jan 2014; accepted 21 Jan 2014; published 6 Mar 2014

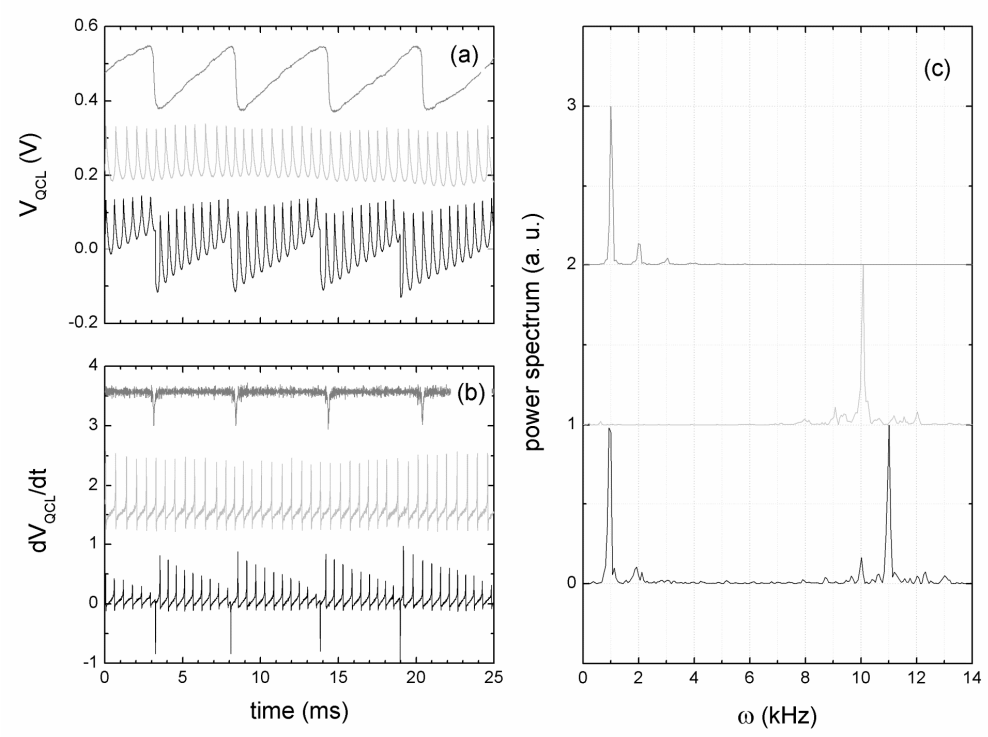

Fig. 2. (a) Representative oscilloscope traces of the interferometric intensity V_{QCL}, (b) its analogue derivative and (c) normalized power spectra of SM signal detected at the junction terminals of the QCL under CW operation. Scope timebase setting: 200 ms/div; sample rate: 2.5 MS/s. Upper trace (gray curve): target T_1 moving in the forward direction at $v_1 = 0.5$ mm/s. Middle trace (light-gray curve): target T_2 moving in the backward direction at $v_2 = –5$ mm/s. Lower trace (black curve): T_1 and T_2 moving in opposite direction at a set velocity of $v_1 = 0.5$ mm/s and $v_2 = –5$ mm/s, respectively.

The middle trace (light-gray curve) in Fig. 2, was recorded while moving only the remote target T_2 at a constant velocity $v_2 = –5$ mm/s (the minus sign indicates the direction of motion towards the laser source). The target T_1 was kept fixed. The resulting SM fringe period in Fig. 2(a) corresponds to a target displacement of $\lambda/2$ in the backward direction, as put in evidence by differentiating the SM waveform (see the pulse polarity in the middle trace of Fig. 2(b)). The power spectrum peaks close to $\omega_2 = 4\pi v_2/\lambda \approx 10$ kHz; higher harmonics are not shown here.

The lower trace (black curve) in the panels shows the combined displacement of both targets T_1 and T_2 moved in opposite direction at a set velocity of $v_1 = 0.5$ mm/s and $v_2 = –5$ mm/s, respectively. The resulting waveform in the time domain clearly exhibits the superposition of the interference fringes given by the concurrent and independent translations of both targets along the optical axis. In addition to the Doppler shifted peaks relative to the motion of the individual targets at ω_1 and ω_2, a major peaks appears in the Fourier spectrum at the sum frequency $\omega_1 + \omega_2$, featuring the intrinsic nonlinearity of the self-mixing interferometer. The relative amplitude of the frequency components depends on the fraction of the back reflected power from each target surface (also called the feedback ratio), regardless of the motion direction, as discussed further in the next section.

Figure 3 shows the experimental evidence of the frequency dependence on the motion direction for a systematic investigation of the target velocity, i.e. for different speed of T_1, keeping T_2 at a constant $v_2 = –5$ mm/s. Particularly, Fig. 3(a) shows the corresponding spectral signature for $v_1 = 3 – 2 – 1 – 0.5$ mm/s, from top to bottom respectively, in the case

#201073 - $15.00 USD Received 8 Nov 2013; revised 1 Jan 2014; accepted 21 Jan 2014; published 6 Mar 2014

of opposite directions of the targets motion. The major peaks occurring at ω_1 and $\omega_1 + \omega_2$ change accordingly, which proves that the spectra of the interferometric signal bear the information about both target velocity modulus and sign.

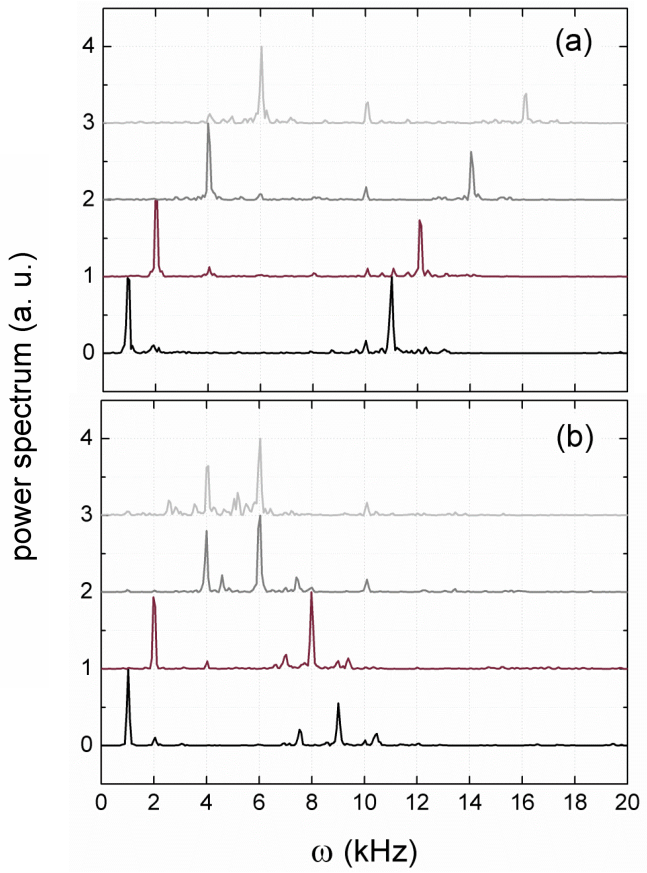

Fig. 3. Normalized power spectra of the experimental interferometric signal V_{QCL} for different velocity of target T_1: $|v_1| = 3 - 2 - 1 - 0.5$ mm/s from top to bottom, respectively. The target velocity $v_2 = -5$ mm/s. (a) opposite direction of the targets motion, with the main peak at the sum-frequency; (b) same direction of the targets motion, with the main peak at the difference-frequency.

Also, the experimental power spectra always contain the same features at $\omega_2 \approx 10$ kHz and at the relative difference-frequency $\omega_2 - \omega_1$, with small peaks nearly buried in the noise floor (i.e. approximately 5–10% the amplitude of the strongest peak in the spectra). Simulations match perfectly the shift of all peaks with speed.

The case of reversed sign of v_1 is shown in Fig. 3(b), proving that this technique is independent on the reciprocal directions of the two translations. By changing the direction of T_1 motion, one observes that the two dominating spectral components in the Fourier analysis become ω_1 and $\omega_2 - \omega_1$, in agreement with simulations shown in Fig. 4(b). The peaks at the difference-frequency $\omega_2 - \omega_1$ shift proportionally to the speed of target T_1, still keeping information about speed of T_2.

3. Theoretical analysis and discussion

In order to interpret the QCL behavior under optical feedback from two targets, we extended the Lang-Kobayashi (LK) model [15] to account for an external dual cavity. This approach was successfully adopted to describe the semiconductor laser dynamics in presence of optical

#201073 - $15.00 USD Received 8 Nov 2013; revised 1 Jan 2014; accepted 21 Jan 2014; published 6 Mar 2014

feedback from multiple reflective surfaces [16] or multiple parts of a single reflecting target [11]. Specifically, we set two coupled nonlinear delayed differential LK equations for the slowly varying field amplitude and the carriers density N. Here, the expression for the quantity ΔN (proportional to variations of the compliance voltage V_{QCL}) was retrieved by solving the LK equations for the stationary states:

$$\Delta N = G\tau_p (N - N_{sol}) = -\frac{2\tau_p}{\tau_c}[k_1 \cos(\omega_F \tau_1) + k_2 \cos(\omega_F \tau_2)] \quad (1)$$

where G is the gain coefficient, N_{sol} represents the carrier density of the solitary laser in absence of feedback; τ_p and τ_c are the photon lifetime and the cavity roundtrip time in the laser cavity (typical value in a QCL: 100 ps and 40 ps, respectively); $\tau_i = 2L_i/c$ (i = 1, 2) is the round trip time in the cavity formed by the laser exit facet and the target T_i. The feedback contribution from the reflectors is parameterized by the coupling coefficients k_i. The laser frequency in presence of feedback, ω_F, is solution of the transcendental equation:

$$\omega_F = \omega_0 - \frac{k_1}{\tau_c}[\alpha \cos(\omega_F \tau_1) + \sin(\omega_F \tau_1)] - \frac{k_2}{\tau_c}[\alpha \cos(\omega_F \tau_2) + \sin(\omega_F \tau_2)] \quad (2)$$

where $\omega_0 \approx 300$ THz is the solitary laser frequency and the linewidth enhancement factor α has a typical value of 1–2 in a MIR QCL [2].

Setting $L_i = L_{0i} + \tau v_i$; $A_i = 2L_{0i}\omega_F/c$; and $\omega_i = 2|v_i|\omega_F/c$ in Eqs. (1) and (2), we get:

$$\Delta N = -\frac{2\tau_p}{\tau_c}[k_1 \cos(A_1 \pm \omega_1 t) + k_2 \cos(A_2 \pm \omega_2 t)] \quad (3)$$

$$\omega_i = \frac{2|v_i|}{c}\left\{\omega_0 - \frac{k_1}{\tau_c}[\alpha \cos(A_1 \pm \omega_1 t) + \sin(A_1 \pm \omega_1 t)] - \frac{k_2}{\tau_c}[\alpha \cos(A_2 \pm \omega_2 t) + \sin(A_2 \pm \omega_2 t)]\right\} \quad (4)$$

where L_{0i} denotes the cavity length at time t = 0 and the signs + and – correspond to positive and negative target velocities v_i, respectively.

From the transcendental character of Eq. (4), it derives that the quantity ΔN given by Eq. (3) does not represent a linear superposition of two cosine functions with constant frequency. The existence of frequency-mixing terms in the power spectrum of ΔN is rather expected. Note also that in the derivation of Eqs. (1)-(4), the perturbation term associated with multiple reflections in the cavity between the two targets was neglected, for instance by assuming that the targets reflectivity was much smaller than the reflectivity of the semiconductor laser exit facet, as done in [16]. Nonetheless, we have easily verified that the inclusions of such a correction term do not alter the main results here discussed and in particular, the interpretation provided for the appearance of peaks at the sum/difference frequency in the power spectrum of ΔN, hence in the power spectrum of the signal V_{QCL}.

In Fig. 4(a) the calculated V_{QCL} for the experimental value of the two targets velocities is plotted, in excellent qualitative agreement with the measurements shown in Fig. 2(a) (see black curve). Figure 4(b) shows the associated normalized Fourier spectrum, where two dominating peaks can be observed: the peak A at the low frequency $\omega_1 \approx 1$ kHz (i.e., corresponding to the velocity $v_1 = 0.5$ mm/s) with the overtones to the right, and the peak B at

#201073 - $15.00 USD Received 8 Nov 2013; revised 1 Jan 2014; accepted 21 Jan 2014; published 6 Mar 2014

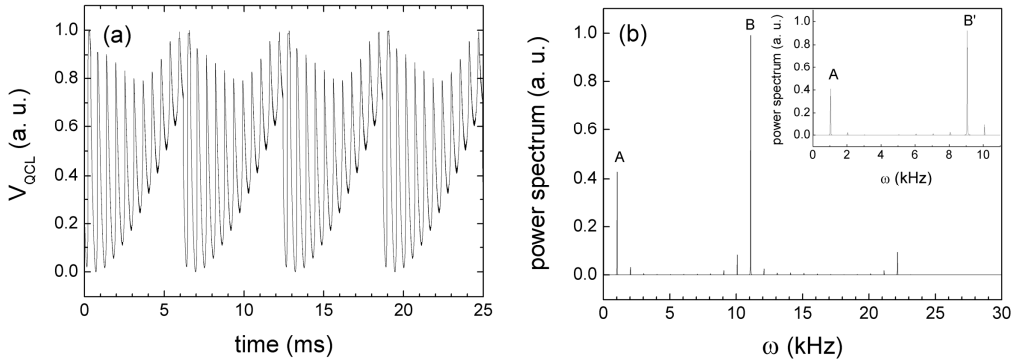

Fig. 4. Numerical results. (a) Time trace and (b) normalized power spectrum of the interferometric signal V_{QCL} for feedback strength coefficients: k_1 = 0.03 and k_2 = 0.025, respectively. Target velocity: v_1 = 0.5 mm/s; v_2 = –5 mm/s. The other parameters are given in the text. The major peak at ≈11 kHz corresponds to the sum-frequency $\omega_1 + \omega_2 = 4\pi(v_1 + v_2)/\lambda_F$. Inset of Fig. 4(b): same parameters, but the motion direction of the target T_2 is reversed (i.e., v_1 = 0.5 mm/s and v_2 = 5 mm/s). The major peak is now at $\omega_1 - \omega_2$.

the sum-frequency $\omega_1 + \omega_2 \approx 11$ kHz. The spectrum in Fig. 4(b) also shows secondary Fourier component peaked at $\omega_2 \approx 10$ kHz, corresponding to the target velocity v_2 = –5 mm/s. The inset of Fig. 4(b) refers to the same case (i.e. same feedback coefficients) but with reverse velocity v_2 = 5 mm/s. Accordingly, the dominant peak at high-frequency B' corresponds now to the difference-frequency $\omega_2 - \omega_1 \approx 9$ kHz.

Finally, Fig. 5 shows the calculated power spectra for three representative values of the feedback strength coefficient k_1 and k_2, keeping constant the ratio k_1/k_2. Simulations prove that the relative amplitude of the main peaks at ω_1, ω_2 and at their sum/difference frequency is dependent on the feedback coefficient k_i. Specifically, the nonlinear frequency mixing in the interferometric spectra emerges at higher feedback levels, and allows to retrieve both target velocity modulus and sign. By decreasing the feedback strength to values typically tolerated by a stable diode laser [1], the spectra show a dominant signature only at the frequency ω_1 and ω_2 (see lower trace in Fig. 5), with negligible sum/difference frequency components.

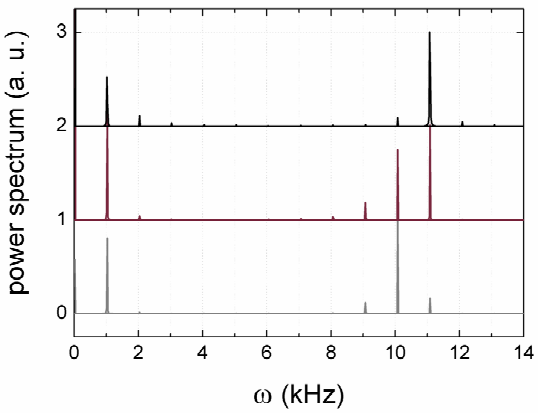

Fig. 5. Numerical results. Normalized power spectrum of the interferometric signal V_{QCL} for feedback strength coefficients: k_1 = 0.025 and k_2 = 0.03 (upper trace), k_1 = 0.012 and k_2 = 0.015 (middle trace), k_1 = 0.006 and k_2 = 0.007 (lower trace), respectively. Target velocity: v_1 = 0.5 mm/s; v_2 = –5 mm/s. For decreasing feedback strength the spectra show a dominant signature only at the frequency ω_1 and ω_2. Same holds if the motion direction of the target T_2 is reversed (not shown here).

#201073 - $15.00 USD Received 8 Nov 2013; revised 1 Jan 2014; accepted 21 Jan 2014; published 6 Mar 2014

4. Conclusion

The simultaneous displacement of two independently moving targets has been measured through nonlinear frequency mixing in a QCL-based interferometer where local oscillator, mixer and detector are combined in a single laser. To access the intrinsic nonlinearity of the fed-back active medium, the QCL stability against strong optical reinjection is here exploited. The QCL in the common-path optical interferometer acts for both the source and the detector of the infrared radiation. The experimental results are in excellent agreement with the numerical simulations based on the Lang-Kobayashi equations upon extension to match multiple external cavities. The collinear arms of the interferometer are terminated by plastic surfaces and can be ultimately generalized to a series of multiple targets semi-transparent to the QCL radiation. In the same configuration, QCLs may be used to determine the distribution of relative velocities in a microfluidic flow channel (i.e. blood flow, particle sizing, etc.). The realization of an integrated QCL in the MIR for differential speed measurement could open new perspectives in lab-on-chip applications. Resonant frequency sensing as well as intracavity or waveguide chemicals detection would greatly benefit by monolithically incorporating onto a single chip the detector functionality within the QCL cavity itself. Also, the thermal expansion of an external cavity could be detected with a flexible membrane replacing the front surface, and the range of detection may be further enhanced by resonant tuning the absorption line of a chemical filling the cavity to the QCL emission wavelength, the latter covering the entire spectral region from mid-infrared to terahertz.

Acknowledgments

The authors acknowledge partial financial support from MIUR – PON01-2238, PON02-0576 INNOVHEAD and MASSIME. The author L.L.C. and M.B. acknowledge funding by National Firb Project PHOCOS (Project n. RBFR08E7VA). The author wish to acknowledge S. Alamri for contributing with useful discussion to the data analysis.

#201073 - $15.00 USD Received 8 Nov 2013; revised 1 Jan 2014; accepted 21 Jan 2014; published 6 Mar 2014